Chapter 7

Tribological Aspects of Graphene-Aluminum Nanocomposites

Prashantha Kumar H.G. and Anthony Xavior M.

Additional information is available at the end of the chapter

http://dx.doi.org/10.5772/67475

Abstract

Graphene is a new class of material in carbon group with strong sp^2—hybridized 2D-sheet like nanomaterial. In order to make an effective utilization of their astounding properties, they are currently used in the form of reinforcements in various proportions in metals and its alloys to fabricate the nanocomposites. Graphene is incorporated in oil and grease at nano range that results in higher load-carrying capacity compared with that of raw grease and oils without additives, which shows that graphene possesses self-lubricating capacity. Graphene is a planar sheet-like structure (2D), with more contact surface area in the developed composites that can make them suitable for industrial applications with well-established tribological performance. The novelty of this work focuses on the role of graphene addition in enhancing the wear performance aluminum composites to replace the conventional materials by graphene composite combinations. The current chapter explains the processing and tribological performance of graphene-aluminum composites and its effect with various hybrid combinations of MWCNT/SiC/Al_2O_3. Dispersion of graphene is carried out through ultrasonic liquid processor followed by ball-milling aluminum powder. Thus prepared precursors are vacuum-pressed and microwave-sintered. Graphene in the nanocomposites has resulted in significantly improving the tribological properties, where it gives the wear resistance by creating a solid, lubricant layer between the sliding surfaces.

Keywords: graphene, aluminum, nanocomposites, tribology

1. Introduction

Recent research advancements in the field of materials, development of strengthened materials without compromising weight factor, are very much fascinating. Due to evolution

in the materials and processing methods, it is required to study the new class of materials and its unusual blends to improve the properties [1–3]. The significance of composites materials technology is the conglomeration of important features of base metals/matrix and the reinforcements. The technology enables achieving high-strength materials without losing the ductility and density, besides, overcoming the drawbacks of base materials by providing viability to add one or more high-strengthened particles and platelets. The necessity for mending the various properties and improved tribological performance will be governed by its applications in addition to various operating conditions [4, 5]. Most of the metal matrix composites are fabricated through ductile materials such as titanium, copper, aluminum, nickel, and its alloy. Such composite materials are extensively taking a role in miniature components of automobile, defense, and huge aerospace structural applications [6, 7]. Ceramic particulates such as silicon carbide, alumina, and boron nitride are the commonly employed reinforcements for the metal matrix composites (MMCs) [8, 9]. The particulate reinforcement trend gave rise to enhanced material properties under appropriate contents that are processed through advanced fabrication techniques compared with its monolithic [10]. Further, MMCs can be sorted out according to the type of reinforcements, namely whiskers (fibers), platelets, or particulates and its physical form with continuous and orientation configurations. In general, whiskers-reinforced and continuous fiber MMCs with advanced fabrication techniques become a promising cost-effective and light-weight engineering material from the past decades [11, 12]. In the recent years, the trend of research is on combinations of advanced materials and new forming methods to synthesis metal matrix composites (MMCs). However, substantial improvement of the aluminum and its alloy-based composites has conquered various manufacturing and industrial sectors. Further, these composites have been widely adapted in various aerospace and automobile industries because of light weight and high strength to weight ratio with improved thermal and electrical properties that are processed through the classical ingot (casting) route [13, 14].

Currently, demands for alternate materials are massive, mainly in various engineering sectors and military applications to facilitate higher payloads and more economical [15, 16]. In order to attain successful fabrication of this material with enriched properties, various permutations of new and advanced materials with cutting-edge processing method are to be adopted [17, 18]. Particulate technology (powder metallurgy) is one such feasible technology that provides the integration of various novel and new combination of reinforcements that can fuse through innovative processing method. The principal element in any composite material assimilating with nanoparticles comprises homogeneous distribution, type of boundary bond, and the interaction of nano reinforcement [19–21].

The materials' research field had been abstracted to find various carbon and its allotropes as reinforcements. Graphene being 2D-sheet like nanomaterial is endowed with extreme strength (tensile strength 130 GPa) in a carbon group that was coined by Andre Geim and Konstantin Novoselov experimentally during 2004 [22, 23]. Further, graphene is an elementary building block for several graphitic materials such as three-dimensional material graphite, single and multiwalled carbon nanotubes (CNTs, one-dimensional), fullerenes (C60, zero-dimensional) [24]. It is strong sp^2-hybridized 2D-nano scale material (sheet like morphology) that is well recognized for its extreme strength. Moreover, it got inspiring attention because of its exceptional physical and

http://dx.doi.org/10.5772/67475

mechanical properties, which includes elastic modulus (up to 0.5–1 TPa); thermal conductivity (up to 5.3 × 103 Wm^{-1} K^{-1}); tensile strength (up to 130 GPa) in the field of research [25]. **Figure 1** shows a distinctive molecular model of single-atomic-layer graphene flake with many other graphitic forms. Carbon nanotubes (CNTs) also have emerged as materials with unique properties greater than those of any available conventional material [26]. Carbon nanotubes (defect-free), both multiwalled nanotubes (MWNTs) and single-wall nanotubes (SWNTs) have superior tensile strengths (~90 GPa) and elastic modulii (~0.6 TPa). Carbon nanotube (CNT), graphite, and fullerenes were used in base metals such as Al, Cu, Mg, and their alloys [27, 28]. Some of the results are found to have significant improvement in the mechanical properties on CNT-reinforced MMCs. But these composites subjecting to various challenges, including uniform distribution of CNTs in the matrix materials, lower surface contact area, and wettability, have been among the major concerns [29].

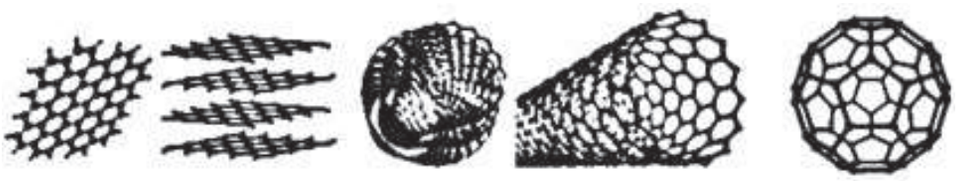

Figure 1. Structure of allotropes of carbon: (a) Graphene; (b) Graphite; (c) MWCNT; (d) SWCNT; (e) Fullerence.

Initially, graphene preparations are carried out by breaking the graphite into graphene through a liquid phase exfoliation or mechanical cleavage method. An other equally common method is chemical vapor deposition (CVD) [30]. Compared to other physical forms of carbon materials such as CNTs and graphite, graphene has been anticipated to outperform its competitors due to its distinctive properties and has great latent in developing the nanocomposites. So the requirement was limited to microscale aggregate without concerning about mechanical properties and strengths. But the excellent mechanical properties of carbon-based graphene are yet to be taken advantage of in metal and its alloy matrix composites [31, 32]. The challenges in synthesis and production of its alloy—graphene composites remain similar to that of ceramic-graphene system or polymer-graphene systems, which have poor dispersion, agglomeration, and individually exfoliated graphene in the matrix. An additional challenge for metal and its alloy—graphene composites could be the unusual reactions at the interfaces [33]. Aluminum-graphene and various aluminum/CNT/SiC/Al_2O_3 combination composites are fabricated through advanced processing techniques such as spark plasma sintering (SPS), mechanical alloying, powder metallurgy (PM), hot press and extrusion [34, 35], melt-blending [36], and hot isostatic pressing (HIP) [12]. But the important factor is the mechanism of various planar/tubular/spherical-shaped structured reinforcement bonding, specific surface area (SSA), and its proposed structural and tribological performances [37]. Further, hybrid combinations of graphene are combined with other reinforcements, and its effect on various mechanical and tribological performances of aluminum matrix is not addressed so far. The current chapter deals with the composite made out of aluminum reinforced with the graphene and its hybrid combinations with CNT/SiC/Al_2O_3 that are processed through ultrasonic liquid processor, ball milling, and consolidated through vacuum hot press followed by microwave sintering. Thus developed composites are

tested for its tribological potential. Comparison and analysis are carried out to explore the effect of friction, wear, and structural damage on the added carbon allotropes during various testing conditions.

2. Processing and fabrication technique of graphene-aluminum composites

Figure 2 shows the morphology of aluminum, SiC, Al_2O_3, MWCNT, and graphene, which is characterized through scanning electron microscope. **Figure 2(a)** and **(b)** shows the TEM micrographs of graphene and MWCNT, respectively. Graphene is in flake form, single-layered morphology in which the layers are stacked upon each other. **Figure 2**(c–e) shows the aluminum, SiC, Al_2O_3, respectively. Aluminum powders that are produced through gas atomization method were procured commercially with a density of 2.7 g/cm^{-3}. Also, SiC particles with a density of 3.20 g/cm^{-3}, Al_2O_3 particles with a density of 3.8 g/cm^{-3}, CNT with a density of 1.6 g/cm^{-3} and graphene with average platelets (flake) size >10 μm, and a density of 1.5–2.0 g/cm^{-3} are considered for the fabrication as reinforcements. Aluminum-graphene nanocomposites with hybrid combinations are produced through a number of ways. At the first step, dispersion of graphene is carried out through an ultrasonic dispersion method with various weight percentages. SiC/CNT/Al_2O_3 was added separately to a solvent containing graphene that is dispersed in acetone. Dispersion (ultrasonication) is carried out until it turns to complete block solution indicating that no graphene sediments were left in the beaker also; all flakes are individually exfoliated. Further, graphene mixtures are dried in hot air oven and subjected to ball milling. Ball milling is carried out for 90 min with the ball mill ratio 16:1 at 200 rpm rotating speed for hybrid combination graphene weight fraction precursor. Encapsulation and homogeneous dispersion of graphene on SiC/Al_2O_3 and homogeneity of mixture are achieved at optimized processing parameters. **Figure 2**(f–h) shows the portion of the ball-milled graphene-SiC/Al_2O_3 powder mixtures that confirm the encapsulation of SiC and Al_2O_3, respectively. Apparent density of aluminum, SiC, Al_2O_3, MWCNT, and graphene is listed in **Table 1**, which are measured according to ASTM B703-10 using Arnold density meter, and tap density is carried out according to ASTM B527-14 by tapping apparatus giving 250 taps under dry conditions. Aluminum metal powder is added parallel to ball-milled hybrid-graphene precursors, and ball-milling process is continued with the same milling ratio for another 30 min. After this, the precursor (mixture of graphene and its hybrid combinations) is dried in hot air oven for 24 hours. Further, precursors are consolidated in vacuum hot press at 240 N/mm^2 in chromium hot-work tool steel (40–48 HRC die case, at 480°C). Boron nitride spray (Momentive Performance Materials Inc. USA) type lubrication is used as a lubricating agent between the precursor and the die walls. Thus prepared compacts are (each comprising two sets) subjected to microwave sintering at 510°C in a nitrogen inert gas (flushing) atmosphere for 30 min followed by furnace cooling to attain room temperature. The process followed for the synthesis of aluminum-graphene and its hybrid combinations is illustrated in **Figure 3**.

http://dx.doi.org/10.5772/67475

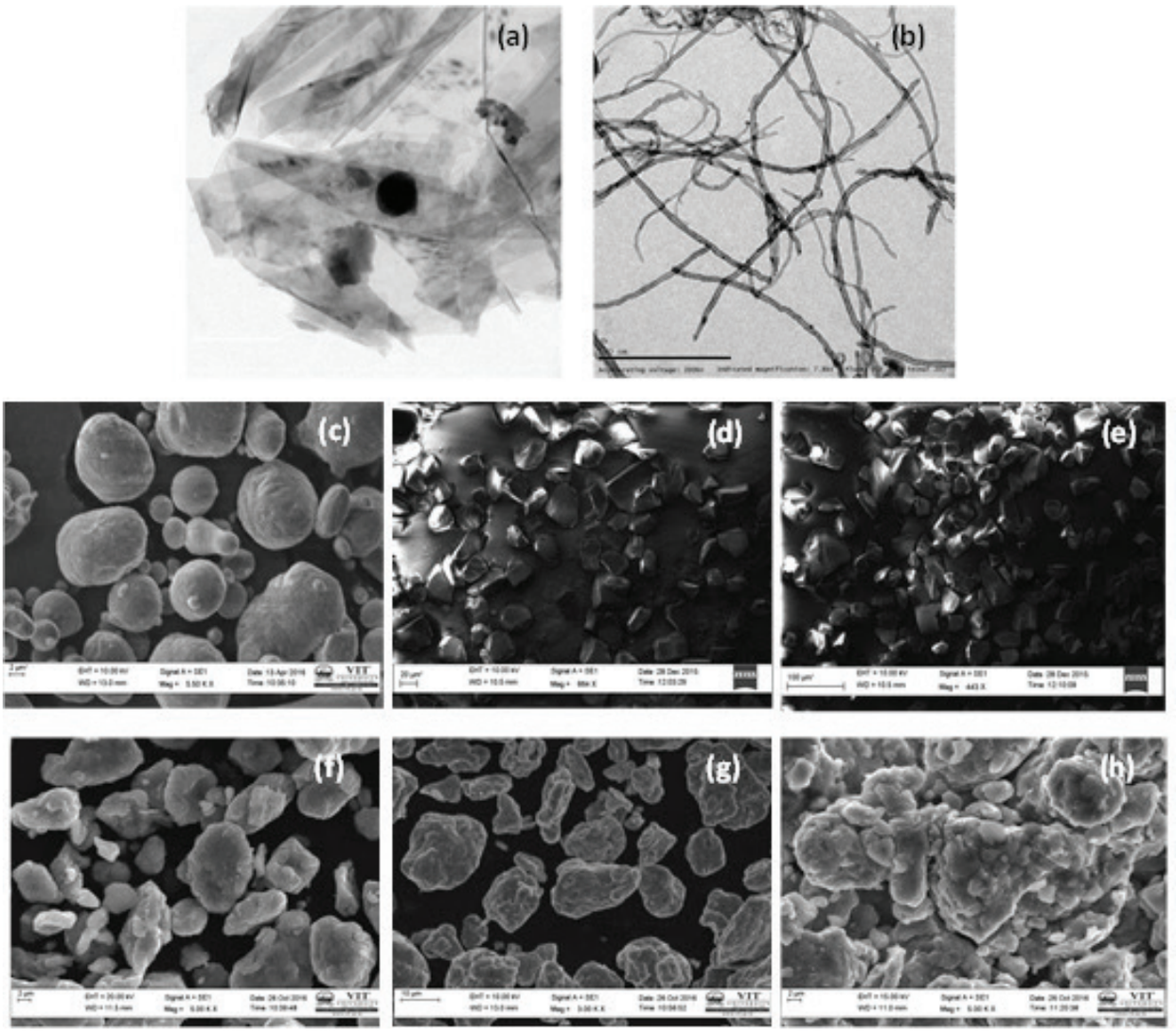

Figure 2. TEM image of (a) Graphene (b) CNT; SEM image (c) Aluminum powder morphology (d) SiC and (e) Al_2O_3; Ball-milled aluminum with (f) MWCNT (g) SiC and (h) Al_2O_3; precursors.

(g/cm^3)	Apparent density (ρ_a)		Tap density (ρ_t)
	Max	Min	
Graphene	0.088 ± 0.002	0.071 ± 0.002	0.1288 ± 0.02
AA 6061	1.118 ± 0.05	0.95 ± 0.05	3.68 ± 0.05
SiC	2.600 ± 0.06	1.9 ± 0.04	3.83 ± 0.03
CNT	0.076 ± 0.002	0.069 ± 0.002	0.1288 ± 0.02
Al_2O_3	2.580 ± 0.06	2.0 ± 0.04	3.98 ± 0.03

Table 1. Measured apparent and tap density values.

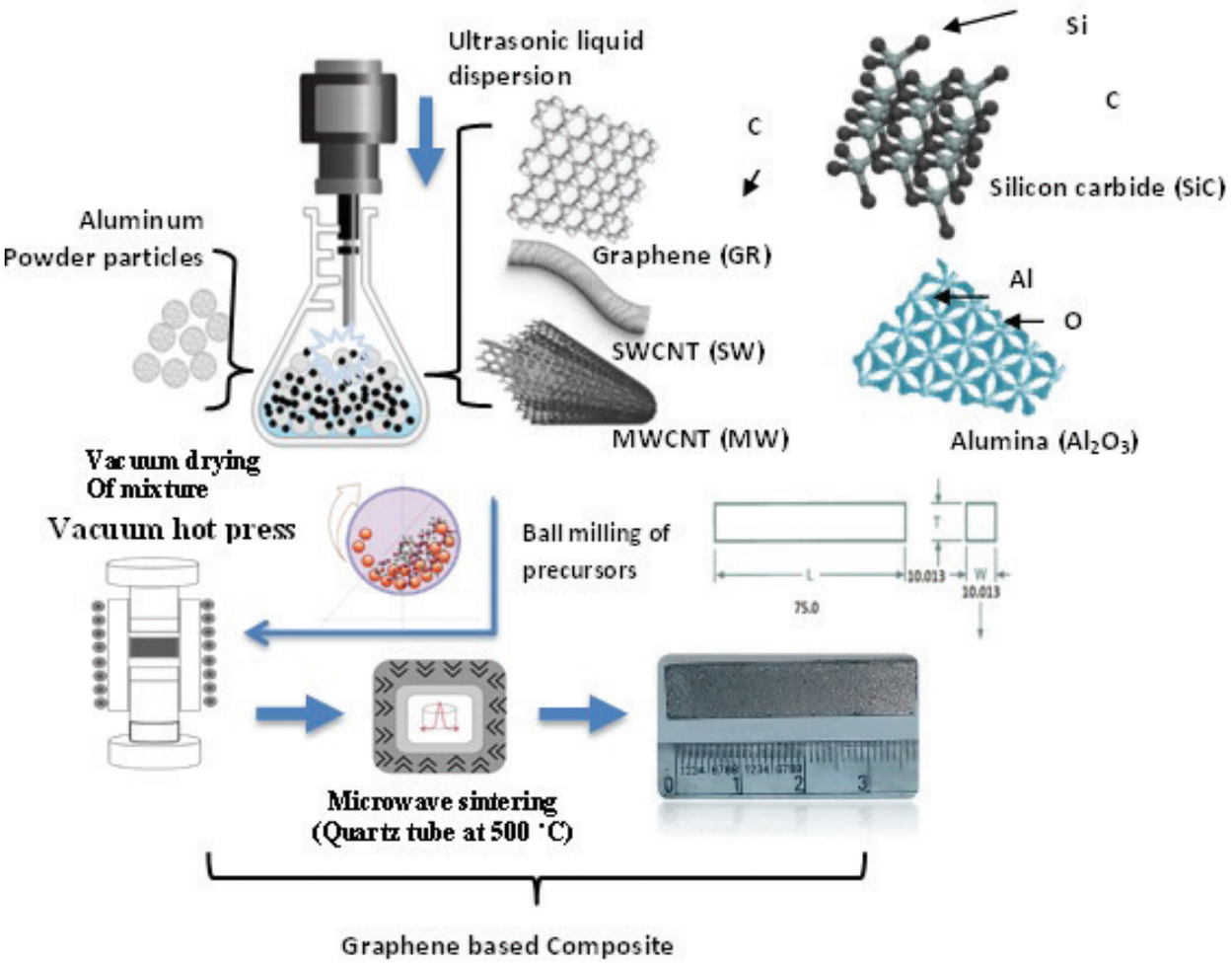

Figure 3. Powder processing through ultrasonic liquid processor and ball milling followed by vacuum hot press and microwave sintering.

3. Testing methods

Vickers hardness values are measured for all aluminum-graphene and other hybrid composite samples using 200 gf after fine polishing of the samples that are sintered at microwave furnace. The mean values of at least five measurements from different areas on the composites sample were taken to analyze. Theoretical densities (g/cm^{-3}) of nanocomposites measured according to the rule of hybrid mixtures (RoHM) relation shown in Eq. (1) and the values of both theoretical and sintered density (g/cm^{-3}) are summarized.

$$D_{\text{Theorerical}} = D_{\text{matrix}} * V_{\text{Matrix}} + D_{\text{Particulate}} * V_{\text{Particulate}} + D_{\text{Graphene}} * V_{\text{Graphene}} \quad (1)$$

where D is the density and V is the volume fraction.

The tribological experiment was carried out according to ASTM G 99-95 standards on pin-on-disc friction and wear testing machine, with disc material: EN-31 steel (hardness: 60HRC). It consists of a pin holder that is connected to the loading lever and measures the wear loss

http://dx.doi.org/10.5772/67475

by LVDT. The fresh specimen is used for each test with a size of 8 mm diameter and 25 mm length prepared by machining. Wear tracks of the disc are polished before and after every wear test using emery paper till it gives a roughness value of 1.6 Ra. The polished pin is cleaned in an ultrasonic bath containing methanol. Mass loss or wear loss values were determined by weighing the samples before and after the test. The surface roughness (Ra), max peak (Rp), and max valley (Rv) values are measured through a surface roughness tester.

4. Microwave sintering mechanism of graphene-aluminum nanocomposites

In aluminum nanocomposites, increase in strength during solid-state sintering (microwave sintering) is attributed to diffusion type of material transport mechanism that takes place due to a vacancy concentration gradient. When the electromagnetic wave is incident on the nanocomposites, most of it will be absorbed, converted into heat, and partly will be reflected as depicted in **Figure 4**. This phenomenon also depends on temperature and chemical potential gradient. For the effective grain, a large number of high energized movements of atoms should be there at the vacancies, but this movement is inhibited by the graphene creating a barrier against grain growth by wrapping. So densification increases during microwave sintering due to increase in the diffusion rate that is directly proportional to the sintering temperature, and it can be related by Arrhenius equation as shown in Eq. (2).

$$N = N_0 \, e^{\frac{-q}{RT}} \tag{2}$$

where N is the number of vacancy sites, N_0 is the total number of lattice sites, q is the activation energy, RT is the average kinetic energy.

Also, under compressive loading conditions, graphene is subjected to deformation and buckling when it is aligned parallel to compressive load. Further, there is no influence on compressive strength if flakes are aligned perpendicular to compressive load applied. In both the cases, nanocomposites are subjected to more strain rate during deformation compared with monolithic aluminum, and this can be arrested by adding SiC/Al_2O_3 particles (harder particle) in both compressive and diametrical loading conditions. It is also possible to achieve the improved strength when the flake is oriented approximately at 45° to the loading direction. The chances of achieving the strength are possible only in particular directions, but achieving

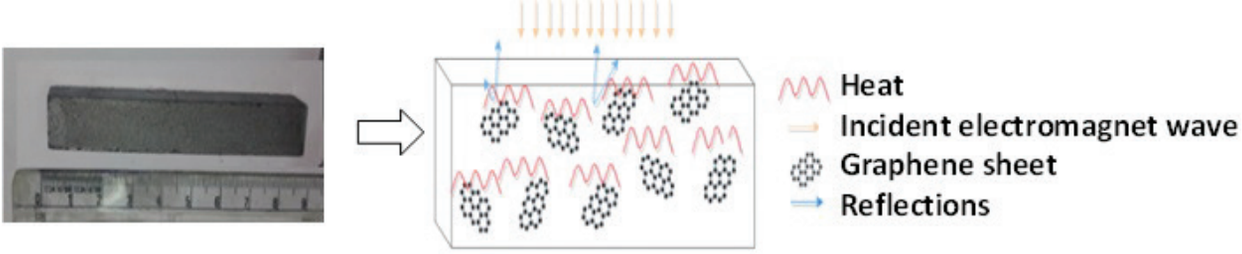

Figure 4. Possible dissipation route of incident electromagnetic wave in the aluminum/graphene composite.

in all directions is quite incredible when graphene alone is considered in the nanocomposites. But combinations of SiC/Al_2O_3 and graphene have advantages in enhancing the strength of the developed nanocomposites. Experiments are repeated on five samples of each compositions and maximum compressive strength achieved is considered for the analysis. It is expected that addition of graphene and SiC/Al_2O_3 leads to dislocation of the pile, resulting in increasing its strengths. Moreover, flake morphology of graphene is contributed in obstructing the particle movement that leads to narrowing the distance between them, and this is found to be the reason for increase in hardness and density.

5. Tribological performances of aluminum-graphene composites

5.1. Effect of graphene

The hardness values of various weight fractions of graphene-based aluminum composites synthesized by uniaxial hot compaction (in mushy state) and microwave sintered are found to have drastic improvements (**Figure 5(a)**) due to addition of graphene and found highest for 0.3 (98 HV), 0.6 (92 HV), and 0.9 (83 HV) weight fractions of graphene compared to aluminum (65 HV). The increase in the hardness confirms the formation of more refined compacted structure [38], and further increase in the hardness can be estimated by rule of mixture, i.e., increase in the graphene content increases the hardness due to reinforcement effect by filling the micro voids [39]. Further, relative density ($\rho_{exp/}\rho_{th}$) of aluminum and all aluminum-graphene composites was above 98%. **Figure 5(b)** relates the wear loss (gms) of pure aluminum and aluminum-graphene nanocomposites with various weight fractions (in weight percentage) of graphene as a function of various load conditions. It is inferred that upon addition of graphene the wear loss decreased self-effacingly. Further, while increasing the graphene content, significant decrease in the wear loss was observed, and minimum wear loss is observed for the 0.3 and 0.6 weight fraction composites. This extensive reduction in the wear loss is attributed to the strengthening of composites by an addition of graphene [40, 41], and its tribological properties form the thin dry lubricant layer between mating metal. This behavior is inconsistent with the work done by the other researchers [42, 43]. While considering the effect of load on the composites, it was inferred that there is an increasing trend of wear loss upon increasing the load. This is due to increase in the corresponding friction values between the mating parts. On the other hand, the presence of more content (≥1.2 wt.%) of graphene may lead to agglomeration, thereby resulting in porosity and cracks that lead to a weakening of structural properties [44]. From **Figure 5(c)**, it is inferred that there is a decrease in the coefficient friction for an increase in graphene content in the composite compared to that of aluminum-base material. The friction value is found to be 0.25–0.35, which is very less compared to aluminum composite friction values viz 0.32–0.39 irrespective of applied normal loads. In general, the friction value depends on the mating materials and relative hardness. Further, the decrease in the coefficient of friction values is attributed to the formation of graphene solid lubricant layer between the wear surfaces, which gives rise to the smooth surface, thereby reducing the contact area [45]. When there is an increase in the normal load, the effective contact area increases between the pin (aluminum-graphene) and the disc (EN-31Steel),

http://dx.doi.org/10.5772/67475

which leads to an increase in the frictional forces. **Figure 5(d)** is the comparative plots of variation of surface roughness (Ra) values with respect to aluminum base and aluminum-graphene composites for various graphene contents. The plots are obtained as a function of load, and it can be inferred that the surface roughness, Ra value is (2.54–1.9 for aluminum, 1.7–1.33 for the aluminum-graphene composites) found to be lesser than that of the base material for all the normal load applications. The addition of graphene has a positive effect, where graphene becomes a sacrificial layer that when smeared (dry lubricant) on the wearing surface leads to a decrease in the max peak, Rp (3.6–2.8 for aluminum, 3.3–2.8 for aluminum-graphene) and max valley Rv (4.1–3.1 for aluminum, 3.5–2.7 for aluminum-graphene composites) values shown in the **Figure 5(e)** and **(f)**, respectively. The decrease in Rp and Rv values leads to fewer asperities contact and in turn produces a relatively smooth surface.

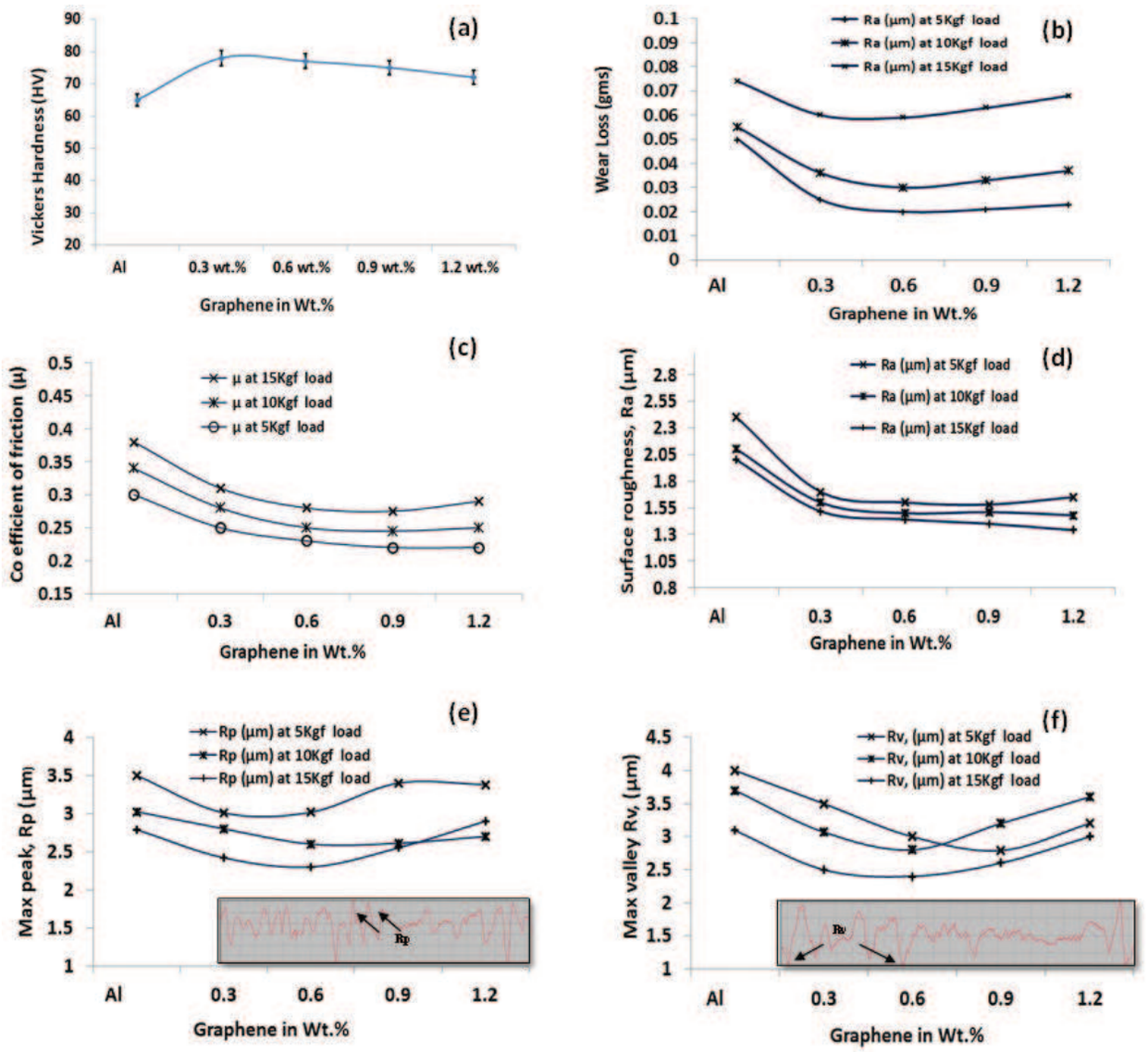

Figure 5. (a) Variation of hardness values; (b) Wear loss; (c) Co-efficient of friction; (d) Surface roughness; (e) Max peak; (f) Max valley with varying the graphene content as a function of load.

Figure 6(a_1–a_5) shows the SEM morphology of worn surfaces immediately after higher normal load conditions (15 kgf) for various aluminum-graphene volume fractions and base under dry sliding conditions. Several macro and deep grooves are noticed in the unreinforced (**Figure 6**(a_1)) compared to graphene-reinforced composites. Further, microgrooves are seen in the aluminum −0.3 wt.% graphene (**Figure 6**(a_2)) and aluminum –0.6 wt.% graphene (**Figure 6**(a_3)) composites. Very few or no grooves are seen on the 0.9 wt.% (**Figure 6**(a_4)) and 1.2 wt.% (**Figure 6**(a_5)) graphene composites. The smeared graphene layer is (puckering effect shown in **Figure 7**) a beneficial (as a dry lubricant) layer that prevents the abrasive wear by protecting the surface same like as seen in carbon nanotubes [46]. It is also expected that at higher volume fractions, graphene may pull out due to more loosely packing/weak bonding with the matrix, which creates thin graphene film that is unnoticeable.

The SEM analysis of wear debris is projected in **Figure 6**(b_1–b_5). Most of the debris are in spherical shape (looks like the metallic particle) (**Figure 6**(c_1)), which are fragments of aluminum under dry wear conditions. **Figure 6**(b_2–b_4) predicts few metallic and more sheets rolled up morphology due to the presence of graphene and tangential/shear force on embedded metal-graphene layers that are formed on the tribo surface. Further, it confirms the formation of solid lubricating layer and failure, subsequently. **Figure 6**(b_5) shows the clear sheet morphology made of fragments of graphene that are detached, crushed/embedded and that which contributed to the formation of the solid film between the mating parts [47].

Figure 6(c_1–c_5) shows the effect of graphene on the surface morphology under dry wear conditions that are analyzed through AFM imaging. The samples without the graphene content (**Figure 6**(c_1)) show more asperities penetration depth compared to aluminum-graphene composites (**Figure 6** (c_2–c_5)) that are tested under 15 kgf load condition. The wear rate of the sample is directly proportional to asperities depths, which are seen more in the unreinforced aluminum compared to aluminum-graphene composites (small rough spots), and it is in good agreement with the current research work. Further, the formation of graphene film prevents the welding of asperities by local heating, which may lead to the formation of scoring or scuffing by providing smooth and low surface roughness.

Marginal change of wear rate trends is observed (**Figure 8(a)**) as a function of sliding speed, and it is not in good agreement with the other researchers work [48, 49] for the aluminum-graphene (various weight fractions) composites that are carried out under different (0.4, 0.8, and 1.2 m/s) sliding speed. But the addition of graphene always brings down the wear rates by lowering the frictional heat, and it is observed to be optimum at 0.6 weight fraction for all the sliding speed conditions. Also, it can be noticed that the wear debris on wearing surface is more on increasing the sliding speed. Most debris are seen as flakes and that may give rise to rubbing abrasion media, which lead to insignificant increasing on the wear rate upon increasing the sliding speeds. Further accumulation of debris leading to agglomeration that was found at some points tested under high sliding speed. The comparison of surface roughness suggests that addition of graphene decreases the roughness values, and it has less significance to the increase in the sliding speed. The occurrence of plastic deformation together with debris morphology indicates the ploughing wear. These are seen at higher sliding speeds (1.2 m/s) and higher graphene concentration (1.2 wt.%)

http://dx.doi.org/10.5772/67475

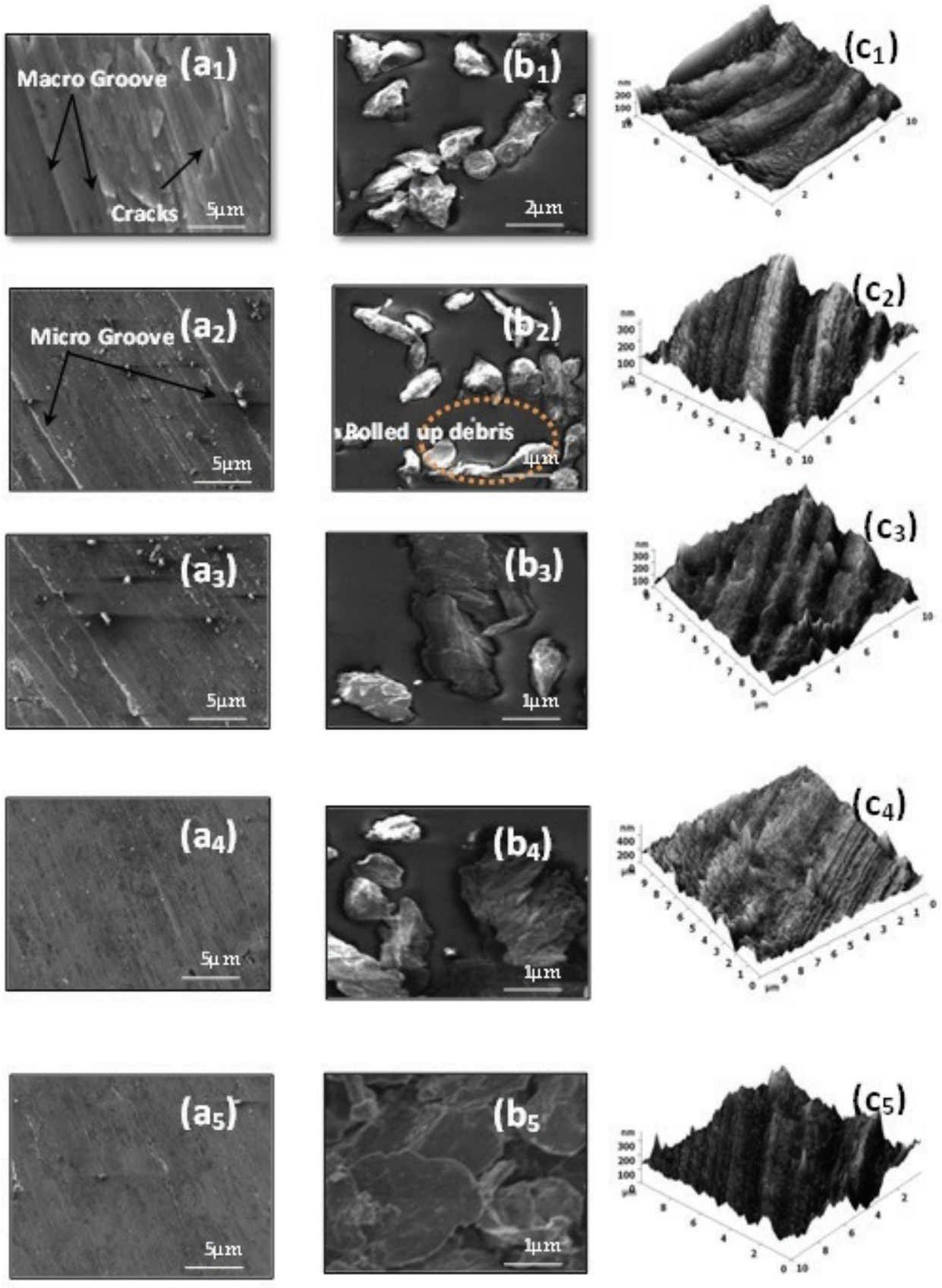

Figure 6. (a) SEM of worn out surface; (b) SEM of wear debris; (c) AFM image of worn out surface.

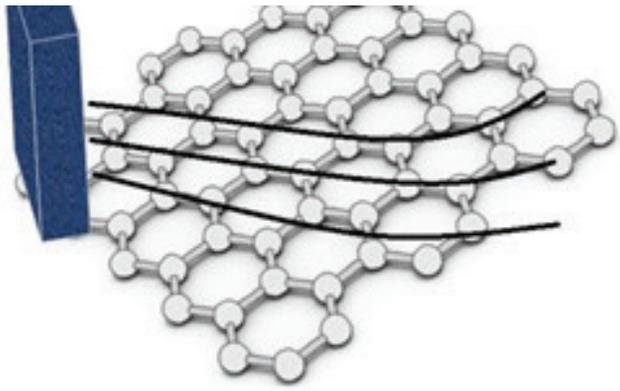

Figure 7. Puckering influence on hexagonal carbon sheet.

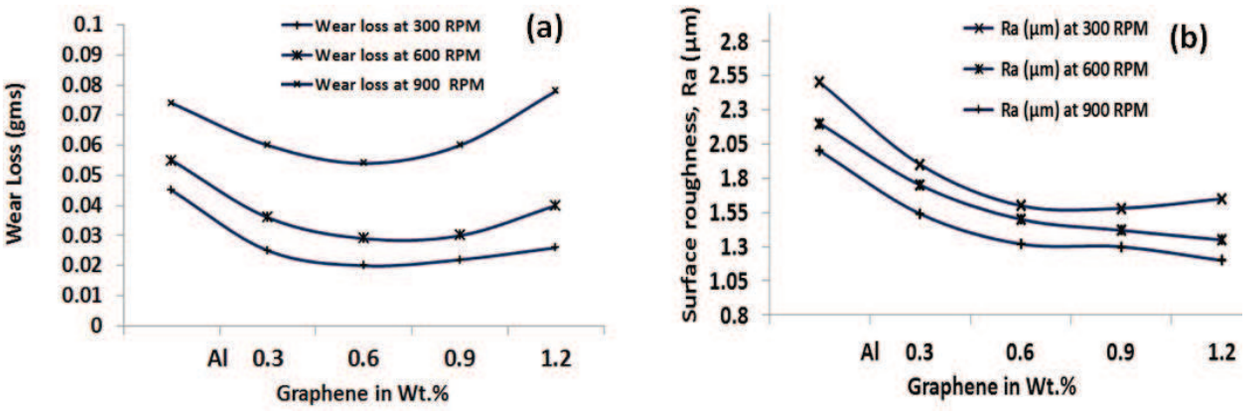

Figure 8. (a) Wear lass; (b) Surface roughness with varying graphene content as a function of speed.

composites (**Figure 9(a)**). Although more black shades on the rubbed surface confirm the presence of more graphene content that peels off and accumulates during rubbing at high frictional force and also same sheet-like debris are seen in **Figure 9(b)**.

5.2. Effect of graphene hybrid combinations with MWCNT

The improvement in the hardness confirms the formation of a more refined compacted structure for the graphene and graphene/MWCNT ball-milled precursors. Addition of graphene acts more as a grain growth inhibitor compared to MWCNT due to difference in the specific surface areas (SSAs) leading (pinning at boundaries) to formation of fine grains that increase the hardness. Further, the combination of graphene/MWCNT leads to slippage and clustering that leads to least effect on grain growth formation within the composites. But the combination of graphene/MWCNT processed through ball milling leads to breaking of MWCNT clustering, flattening, and embedding on the aluminum particulate through plastic deformation. In addition, during ball milling, graphene flakes get flattened and become a monolayer, and interatomic distance between carbon atoms will increase and get packed by matrix atoms [50, 51].

http://dx.doi.org/10.5772/67475

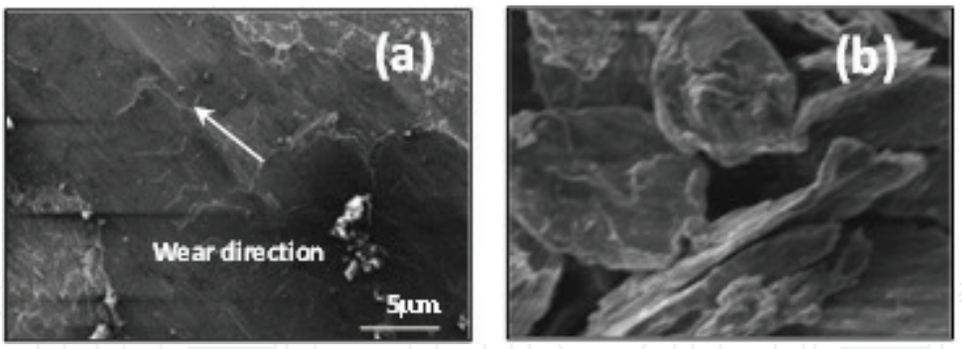

Figure 9. SEM of (a) Worn out surface; (b) Wear debris.

It is inferred that upon addition of graphene on aluminum and aluminum-graphene/MWCNT (flattened) combinations will give the least wear loss compared to monolithic, MWCNT, and aluminum-graphene/MWCNT (tubular) composites. This extensive reduction in the wear loss is attributed to the strengthening of composites by a combination of graphene/MWCNT, processing method, and it is in good agreement with the improved hardness values. Combinations of MWCNT/graphene and MWCNT alone may lead to agglomeration, thereby resulting in porosity and cracks that lead to weakening of structural properties. The friction value is found to be very less for aluminum-graphene/MWCNT composites compared to monolithic aluminum irrespective of applied normal loads. Also, aluminum-graphene/MWCNT (flattened) is found to have least friction values compared to other combinations. This difference in the coefficient of friction values is attributed to the formation of graphene and flattened MWCNT during ball milling as solid lubricant layer between the wear surfaces. In general, the friction value depends on the mating materials and relative hardness. The effective contact area increases between the pin of various aluminum-graphene/MWCNT composites and the disc (EN-31Steel) due to increase in the normal load that leads to increase in the frictional forces. **Figure 10**(a–e) shows the SEM morphology of worn surfaces immediately after higher normal load conditions (15 kgf) for various aluminum-graphene/MWCNT and base aluminum under dry sliding conditions. Several macro and deep grooves are noticed for the monolithic aluminum (**Figure 11(a)**) compared to various alus. **Figure 11**(b–e) represents the worn-out surface of various aluminum-graphene/MWCNT composites in which the smeared graphene layer and MWCNT (flattened) are a beneficial (as a dry lubricant) layer in the composites, which prevent the abrasive wear by protecting the surface.

From the wear rate and friction coefficient, values of aluminum and aluminum-graphene/MWCNT composites are carried out under different (0.5, 1.0, and 1.5 m/s) sliding speed at a sliding distance of 1200 m and constant applied load (45 N). But the addition of graphene and combination with flattened MWCNT during ball milling has a significant advantage in bringing down the wear rates by lowering the frictional heat. The decreasing trend of wear rate is observed as a function of sliding speed. Also, the embedded graphene and flattened MWCNT give planar edges compared to spherical edge of the CNT in the composites, which are prone to high stress interacting sites. Further, accumulation of debris leading to agglomeration was found at some points tested under high sliding speed. Most debris are seen as flakes and that may give rise to rubbing abrasion media, which lead to insignificant increasing

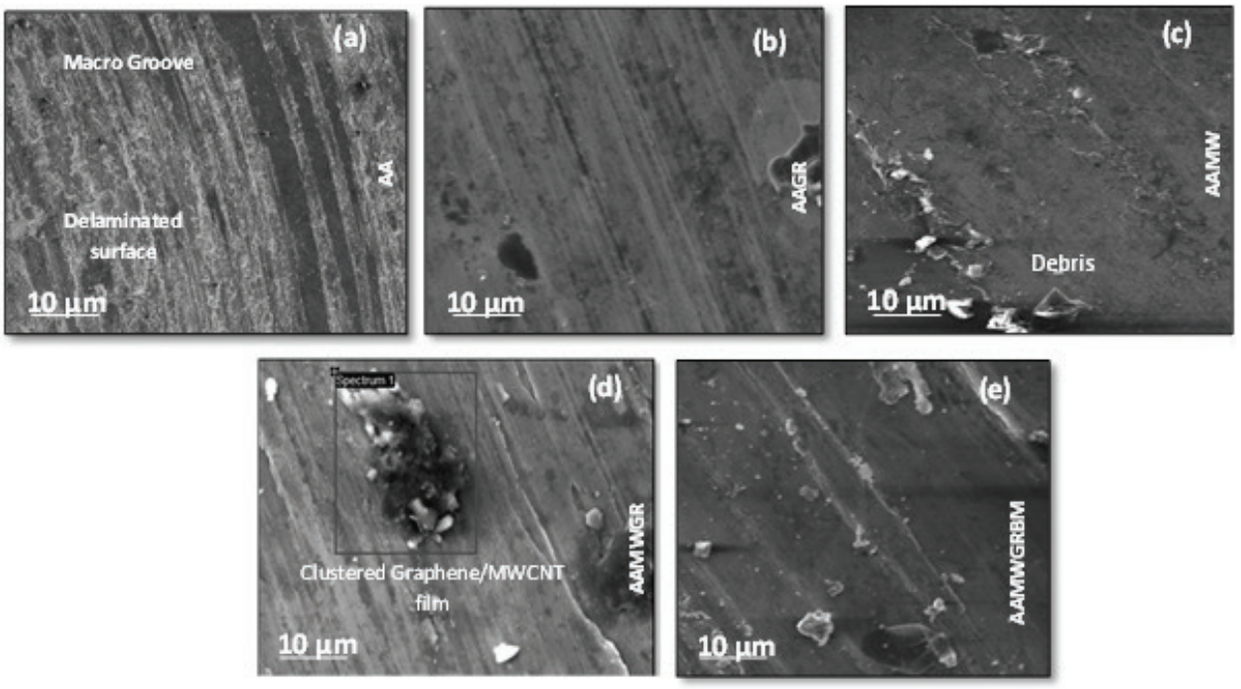

Figure 10. SEM of aluminum-graphene/MWCNT composites worn-out surface varying with the load (N) of (a) AA (b) AAGR (c) AAMW (d) AAMWGR (e) AAMWGRBM.

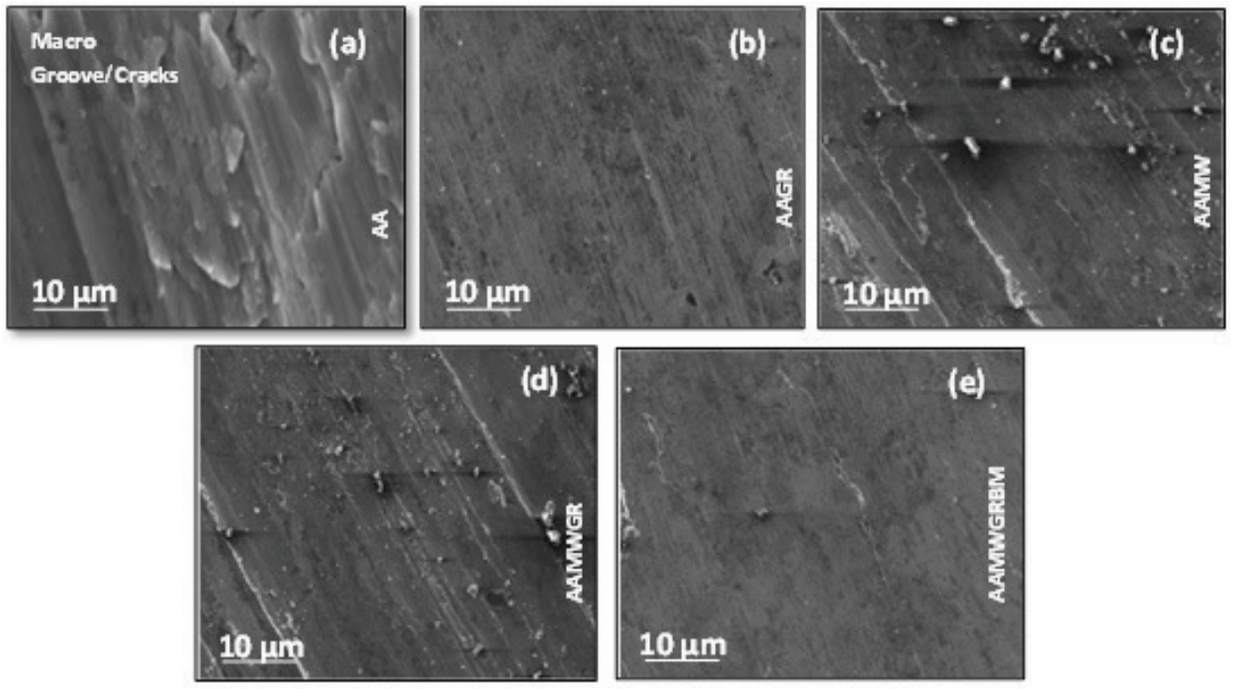

Figure 11. SEM of aluminum-graphene/MWCNT composites worn-out surface varying with the sliding speed (m/s) of (a) AA (b) AAGR (c) AAMW (d) AAMWGR (e) AAMWGRBM

on the wear rate upon increasing the sliding speeds. Most of the wear debris are in spherical shape (delaminated from the wearing surface), which are fragments of aluminum under dry wear conditions. This infers that the deformation is pure by ductile on the surface. Clear sheet morphology made of fragments of sheet graphene and flattened MWCNT combination that are crushed/embedded on tribo surface contributed to the formation of the solid film between the mating parts. Also, few metallic and more sheets rolled up morphology due to the presence of MWCNT, graphene/MWCNT (tubular) combinations, and tangential/shear force on embedded metal on the tribo surface. Further, it confirms the formation of solid lubricating layer and failure subsequently.

5.3. Effect of graphene hybrid combinations with SiC and Al_2O_3

The Vickers hardness values for various concentrations of graphene and SiC/Al2O3 in Al aluminum nanocomposites are found to be improved. This shows that the nanocomposite processed through ultrasonic dispersion and microwave sintering technique exhibits a substantial improvement in micro hardness values compared to base aluminum. It is also being found that the values are superior to the results obtained from other processing methods on the same material [51, 52]. The grouping of SiC/Al_2O_3 and graphene is capable of excellent microwave absorption capacity [53]. Also, when graphene is coated/encapsulated with SiC/Al_2O_3 at lower concentrations (up to 0.5 wt.%) that lead to improved microwave absorption of materials, which ascribed to a change in dielectric parameters. Importantly, graphene and SiC/Al_2O_3 in microscale-ranged particles posses higher surface area that is crucial to make interfacial bonding effective and to enhance the overall densification by minimizing the porosity level.

Addition of graphene and SiC/Al2O3 has a positive outcome in the synthesized composites in which wear loss is found to be reduced self-effacingly. Extensive wear resistance is due to strengthening of aluminum-SiC/Al_2O_3-graphene composites by a combination and addition of graphene and encapsulation with SiC, which is in good agreement with the improved hardness and other properties. Further, coefficient of frictional values is found to be less for the composite compared to aluminum base friction values and is independent of applied normal loading. In general, surface roughness values are constituted by mating materials and hardness (relative). Further, added graphene will act as a solid lubricant between the wearing surfaces, and also the presence of added SiC/Al_2O_3 particles creates the point contact by reducing the third body abrasion. The addition of graphene was found to result in a positive outcome in which coated/encapsulated SiC/Al_2O_3 will become an efficient lubricating layer by smearing on the mating and wearing surface that will create the fine and smooth surface that reduces the roughness values. **Figure 12** shows the optical micrographs of aluminum-graphene-SiC/Al_2O_3 nanocomposites wear out surface, which are rubbed in unlubricated environments. Many macrocracks or grooves are observed (**Figure 12(a)**) for the samples without and very less microsurface (**Figure 12(b)**) on graphene and SiC/Al_2O_3 (**Figure 12**(c–e)) reinforced composites. So it can be concluded that the combination of graphene and SiC/Al_2O_3 with coating/encapsulation leads to enhancing the tribological properties at optimized values.

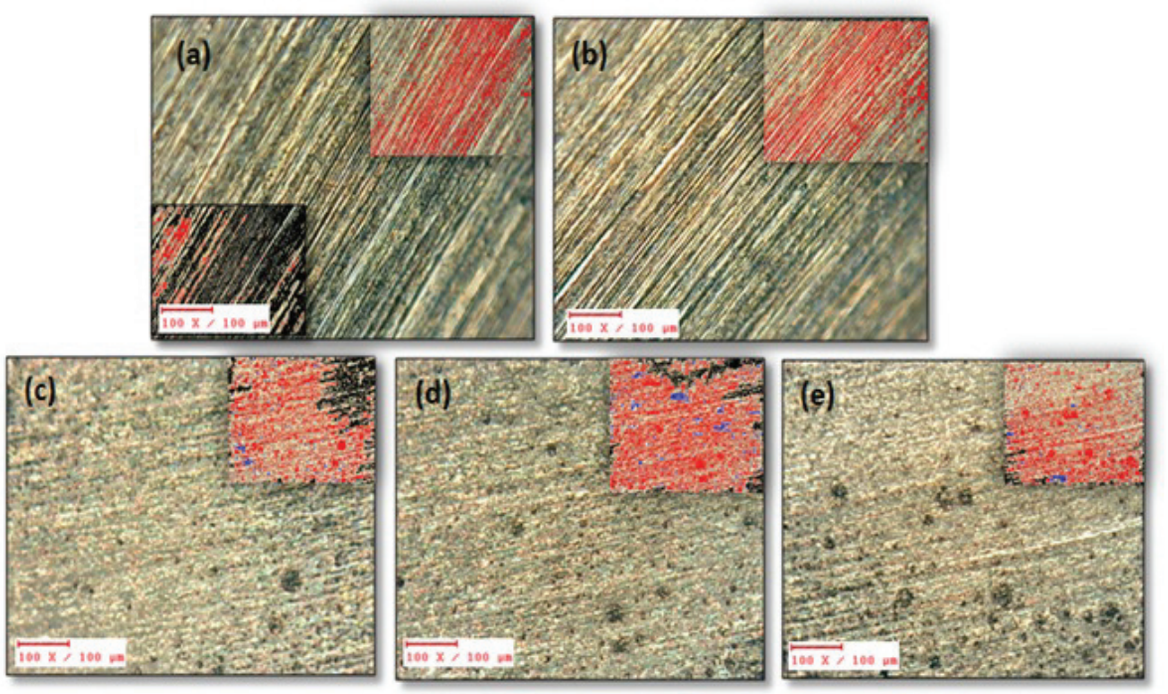

Figure 12. Optical micrographs of worn-out surface of (a) Aluminium (b) Aluminum + Graphene, (c) Aluminum + Graphene + SiC (d) Aluminum + Graphene + Al_2O_3 (e) Aluminum + Graphene + Al_2O_3 + SiC.

6. Conclusion

One of the common engineering research challenges in materials is to determine ways and means to improve the wear resistance between any coupling surfaces, thereby reducing the energy and wear losses. In the current research work, aluminum with graphene is processed separately through vacuum hot press (gives high improved density compacts >98%) followed by microwave sintering successfully. Addition of graphene will provide more number of nucleation's regions. Aluminum-graphene composites are observed to be superior in hardness compared to monolithic material owing to uniform dispersion and higher dispersion strengthening mechanism. Graphene exhibits more grain refinement, which improves the fracture toughness of the composite. This feature has reduced wear losses, and therefore, graphene-reinforced composites are suitable for various tribological applications. The significant differences in the friction coefficients due to high protective nature of graphene will lower the shear force and reduce the material losses. Further, graphene and MWCNT combinations in composite become a sacrificial layer which smeared (dry lubricant) on the wearing surface and enable the self-lubricating properties of aluminum-graphene/MWCNT composites. Graphene/MWCNT (flattened–ball-milled) combination is a favorable tribological application, coupled with improved hardness, strength, and surface roughness values compared to individual MWCNT or graphene/MWCNT (tubular)-reinforced aluminum composites applications, where the component is exposed to wear and friction. Addition of graphene in SiC/Al_2O_3 and encapsulation enables significant improvement in hardness compared to base aluminum. Microwave sintering method can

efficiently increase the diffusion of ions in the composite and thus gear up the sintering process, leading to finer grain growth and the densification. Also, combination of SiC/Al_2O_3 and graphene in the nanocomposites has resulted in significant improvement on tribological properties, where it gives the wear resistance by creating a solid lubricant layer between the sliding surfaces.

Author details

Prashantha Kumar H.G.* and Anthony Xavior M.

*Address all correspondence to: prashanthakumar.hg@gmail.com

School of Mechanical Engineering, VIT University, Vellore, Tamil Nadu, India

References

[1] Surappa MK. Aluminium matrix composites: challenges and opportunities. Sadhana. 2003;**28**(1–2):319-334. DOI: 10.1007/BF02717141.

[2] Hunt W, Herling DR. Aluminum metal matrix composites. Advanced Materials & Processes. 2004;**162**(2):39-44. DOI: AC05-76RL01830.

[3] Prasad SV, Asthana R. Aluminum metal-matrix composites for automotive applications: tribological considerations. Tribology Letters. 2004;**17**(3):445-453. DOI: 10.1023/B:TRIL.0000044492.91991.f3.

[4] Logsdon WA, Liaw PK. Tensile, fracture toughness and fatigue crack growth rate properties of silicon carbide whisker and particulate reinforced aluminum metal matrix composites. Engineering Fracture Mechanics. 1986;**24**(5):737-751. DOI: 10.1016/0013-7944(86)90246-8.

[5] Wang W, Shi QY, Liu P, Li HK, Li T. A novel way to produce bulk SiCp reinforced aluminum metal matrix composites by friction stir processing. Journal of Materials Processing Technology. 2009;**209**(4):2099-2103. DOI: 10.1016/j.jmatprotec.2008.05.001.

[6] Miracle DB. Metal matrix composites – from science to technological significance. Composites Science and Technology. 2005;**65**(15):2526-2540. DOI: 10.1016/j.compscitech.2005.05.027.

[7] Rawal SP. Metal-matrix composites for space applications. JOM. 2001;**53**(4):14-17. DOI: 10.1007/s11837-001-0139-z.

[8] Ibrahim IA, Mohamed FA, Lavernia EJ. Particulate reinforced metal matrix composites—a review. Journal of Materials Science. 1991;**26**(5):1137-1156. DOI: 10.1007/BF00544448.

[9] Shorowordi KM, Laoui T, Haseeb AS, Celis JP, Froyen L. Microstructure and interface characteristics of B_4C, SiC and Al_2O_3 reinforced Al matrix composites: a comparative

study. Journal of Materials Processing Technology. 2003;**142**(3):738-743. DOI: 10.1016/S0924-0136(03)00815-X.

[10] Nair SV, Tien JK, Bates RC. SiC-reinforced aluminium metal matrix composites. International Metals Reviews. 1985;**30**(1):275-290. DOI: 10.1016/j.jmatprotec.2008.05.001.

[11] Tzamtzis S, Barekar NS, Babu NH, Patel J, Dhindaw BK, Fan Z. Processing of advanced Al/SiC particulate metal matrix composites under intensive shearing—a novel Rheo-process. Composites Part A: Applied Science and Manufacturing. 2009;**40**(2):144-151. DOI: 10.1016/j.compositesa.2008.10.017.

[12] Lloyd DJ. Particle reinforced aluminium and magnesium matrix composites. International Materials Reviews. 1994;**39**(1):1-23. DOI: 10.1179/imr.1994.39.1.1.

[13] Hasselman DP, Donaldson KY, Geiger AL. Effect of reinforcement particle size on the thermal conductivity of a particulate-silicon carbide-reinforced aluminum matrix composite. Journal of the American Ceramic Society. 1992;**75**(11):3137-3140. DOI: 10.1111/j.1151-2916.1992.tb04400.x/full.

[14] Zweben C. Advances in composite materials for thermal management in electronic packaging. Journal of the Minerals Metals and Materials Society. 1998;**50**(6):47-51. DOI: 10.1007/s11837-998-0128-6.

[15] Sannino AP, Rack HJ. Dry sliding wear of discontinuously reinforced aluminum composites: review and discussion. Wear. 1995;**189**(1):1-9. DOI: 10.1016/0043-1648(95)06657-8.

[16] Nardone VC, Prewo KM. On the strength of discontinuous silicon carbide reinforced aluminum composites. Scripta Metallurgica. 1986;**20**(1):43-48. DOI: 10.1016/0036-9748(86)90210-3.

[17] Ciftci I, Turker M, Seker U. Evaluation of tool wear when machining SiC p-reinforced Al-2014 alloy matrix composites. Materials & Design. 2004;**25**(3):251-255. DOI: 10.1016/j.matdes.2003.09.019.

[18] Mishra RS, Ma ZY, Charit I. Friction stir processing: a novel technique for fabrication of surface composite. Materials Science and Engineering A. 2003;**341**(1):307-310. DOI: 10.1016/S0921-5093(02)00199-5.

[19] Srivatsan TS, Ibrahim IA, Mohamed FA, Lavernia EJ. Processing techniques for particulate-reinforced metal aluminium matrix composites. Journal of Materials Science. 1991;**26**(22):5965-5978. DOI: 10.1007/BF01113872.

[20] Urquhart AW. Novel reinforced ceramics and metals: a review of Lanxide's composite technologies. Materials Science and Engineering A. 1991;**144**(1–2):75-82. DOI: 10.1016/0921-5093(91)90211-5.

[21] Tjong SC. Novel nanoparticle-reinforced metal matrix composites with enhanced mechanical properties. Advanced Engineering Materials. 2007;**9**(8):639-652. DOI: 10.1002/adem.200700106.

[22] Kumar HP, Xavior MA. Graphene reinforced metal matrix composite (GRMMC): a review. Procedia Engineering. 2014;**31**(97):1033-1040. DOI: 10.1016/j.proeng.2014.12.381.

[23] Jang BZ, Zhamu A. Processing of nanographene platelets (NGPs) and NGP nanocomposites: a review. Journal of Materials Science. 2008;**43**(15):5092-5101. DOI: 10.1007/s10853-008-2755-2.

[24] Yu MF, Lourie O, Dyer MJ, Moloni K, Kelly TF, Ruoff RS. Strength and breaking mechanism of multiwalled carbon nanotubes under tensile load. Science. 2000;**287**(5453):637-640. DOI: 10.1126/science.287.5453.637.

[25] Lee C, Wei X, Kysar JW, Hone J. Measurement of the elastic properties and intrinsic strength of monolayer graphene. Science. 2008;**321**(5887):385-388. DOI: 10.1126/science.1157996.

[26] Young RJ, Kinloch IA, Gong L, Novoselov KS. The mechanics of graphene nanocomposites: a review. Composites Science and Technology. 2012;**72**(12):1459-1476. DOI: 10.1016/j.compscitech.2012.05.005.

[27] Baradeswaran A, Perumal AE. Wear and mechanical characteristics of Al 7075/graphite composites. Composites Part B: Engineering. 2014;**56**:472-476. DOI: 10.1016/j.compositesb.2013.08.073.

[28] Ruoff RS, Lorents DC. Mechanical and thermal properties of carbon nanotubes. Carbon. 1995;**33**(7):925-930. DOI: 10.1016/0008-6223(95)00021-5.

[29] Odom TW, Huang JL, Kim P, Lieber CM. Atomic structure and electronic properties of single-walled carbon nanotubes. Nature. 1998;**391**(6662):62-64. DOI: 10.1038/34145.

[30] Suk JW, Kitt A, Magnuson CW, Hao Y, Ahmed S, An J, Swan AK, Goldberg BB, Ruoff RS. Transfer of CVD-grown monolayer graphene onto arbitrary substrates. ACS Nano. 2011;**5**(9):6916-6924. DOI: 10.1021/nn201207c.

[31] Wang J, Li Z, Fan G, Pan H, Chen Z, Zhang D. Reinforcement with graphene nanosheets in aluminum matrix composites. Scripta Materialia. 2012;**66**(8):594-597. DOI: 10.1016/j.scriptamat.2012.01.012.

[32] Liu J, Yan H, Jiang K. Mechanical properties of graphene platelet-reinforced alumina ceramic composites. Ceramics International. 2013;**39**(6):6215-6221. DOI: 10.1016/j.ceramint.2013.01.041.

[33] Mokdad F, Chen DL, Liu ZY, Xiao BL, Ni DR, Ma ZY. Deformation and strengthening mechanisms of a carbon nanotube reinforced aluminum composite. Carbon. 2016;**104**:64-77. DOI: 10.1016/j.carbon.2016.03.038.

[34] Xu CL, Wei BQ, Ma RZ, Liang J, Ma XK, Wu DH. Fabrication of aluminum-carbon nanotube composites and their electrical properties. Carbon. 1999;**37**(5):855-858. DOI: 10.1016/S0008-6223(98)00285-1.

[35] Park JG, Keum DH, Lee Y. Strengthening mechanisms in carbon nanotube-reinforced aluminum composites. Carbon. 2015;**95**:690-698. DOI: 10.1016/j.carbon.2015.08.112.

[36] Stein J, Lenczowski B, Fréty N, Anglaret E. Mechanical reinforcement of a high-performance aluminium alloy AA5083 with homogeneously dispersed multi-walled carbon nanotubes. Carbon. 2012;**50**(6):2264-2272. DOI: 10.1016/j.carbon.2012.01.044.

[37] Bastwros MM, Esawi AM, Wifi A. Friction and wear behavior of Al-CNT composites. Wear. 2013;**307**(1):164-173. DOI: 10.1016/j.wear.2013.08.021.

[38] Abadi SB, Khavandi A, Kharazi Y. Effects of mixing the steel and carbon fibers on the friction and wear properties of a PMC friction material. Applied Composite Materials. 2010;**17**(2):151-158. DOI: 10.1007/s10443-009-9115-5.

[39] Berman D, Erdemir A, Sumant AV. Graphene: a new emerging lubricant. Materials Today. 2014;**17**(1):31-42. DOI: 10.1016/j.mattod.2013.12.003.

[40] Lee CS, Kim YH, Han KS, Lim T. Wear behaviour of aluminium matrix composite materials. Journal of Materials Science. 1992;**27**(3):793-800. DOI: 10.1007/BF00554055.

[41] Lin J, Wang L, Chen G. Modification of graphene platelets and their tribological properties as a lubricant additive. Tribology Letters. 2011;**41**(1):209-215. DOI: 10.1007/s11249-010-9702-5.

[42] Chattopadhyay PK, Chattopadhyay S, Das NC, Bandyopadhyay PP. Impact of carbon black substitution with nanoclay on microstructure and tribological properties of ternary elastomeric composites. Materials & Design. 2011;**32**(10):4696-4704. DOI: 10.1016/j.matdes.2011.06.050.

[43] Krishnan BP, Rohatgi PK. Modification of Al-Si alloy melts containing graphite particle dispersions. Metals Technology. 2013; 11(1) 41-44. DOI: 10.1179/030716984803274297.

[44] Hocheng H, Yen SB, Ishihara T, Yen BK. Fundamental turning characteristics of a tribology-favored graphite/aluminum alloy composite material. Composites Part A: Applied Science and Manufacturing. 1997;**28**(9):883-890. DOI: 10.1016/S1359-835X(97)00055-9.

[45] Chu HS, Liu KS, Yeh JW. An in situ composite of Al (graphite, Al 4 C 3) produced by reciprocating extrusion. Materials Science and Engineering A. 2000;**277**(1):25-32. DOI: 10.1016/S0921-5093(99)00562-6.

[46] Kim IY, Lee JH, Lee GS, Baik SH, Kim YJ, Lee YZ. Friction and wear characteristics of the carbon nanotube-aluminum composites with different manufacturing conditions. Wear. 2009;**267**(1):593-598. DOI: 10.1016/j.wear.2008.12.096.

[47] Bakshi SR, Keshri AK, Agarwal A. A comparison of mechanical and wear properties of plasma sprayed carbon nanotube reinforced aluminum composites at nano and macro scale. Materials Science and Engineering A. 2011;**528**(9):3375-3384. DOI: 10.1016/j.msea.2011.01.061.

[48] Yousif BF. Design of newly fabricated tribological machine for wear and frictional experiments under dry/wet condition. Materials & Design. 2013;**48**:2-13. DOI: 10.1016/j.matdes.2012.06.046.

[49] Findik F. Latest progress on tribological properties of industrial materials. Materials & Design. 2014;**57**:218-244. DOI: 10.1016/j.matdes.2013.12.028.

[50] Choi HJ, Shin JH, Bae DH. The effect of milling conditions on microstructures and mechanical properties of Al/MWCNT composites. Composites Part A: Applied Science and Manufacturing. 2012;**43**(7):1061-1072. DOI: 10.1016/j.compositesa.2012.02.008.

[51] Bastwros M, Kim GY, Zhu C, Zhang K, Wang S, Tang X, Wang X. Effect of ball milling on graphene reinforced Al6061 composite fabricated by semi-solid sintering. Composites Part B: Engineering. 2014;**60**:111-118. DOI: 10.1016/j.compositesb.2013.12.043.

[52] Leonelli C, Veronesi P, Denti L, Gatto A, Iuliano L. Microwave assisted sintering of green metal parts. Journal of Materials Processing Technology. 2008;**205**(1):489-496. DOI: 10.1016/j.jmatprotec.2007.11.263.

[53] Oghbaei M, Mirzaee O. Microwave versus conventional sintering: a review of fundamentals, advantages and applications. Journal of Alloys and Compounds. 2010;**494**(1):175-189. DOI: 10.1016/j.jallcom.2010.01.068.

IntechOpen